Å. Mo complex: Mo–C(O), 2.00 Å; C–O, 1.15 Å; Mo–C(carbene), 2.30 Å; C(carbene)–N, 1.33 Å; N–H, 1.00 Å; Mo–H, 1.70 Å. Cr complex: Cr–C(O), 1.84 Å; C–O, 1.14 Å; Cr–C(carbene), 2.00 Å; Cr–H, 1.6 Å; C–H, 1.08 Å. All angles at the metal are the ideal values characteristic of each ligand field. All angles within each ligand are standard.

Registry No. 1, 69552-43-8; 2, 71770-16-6; 3, 76748-17-9; 4, 64161-93-9; 5, 91463-01-3; 6, 78128-66-2; 7, 83288-64-6; $H_3Ta(CH_2)_2^{2-}$, 112069-47-3; $H_2Rh(CH_2)_2^-$, 112069-48-4; $(CO)_4Cr(CH_2)_2$, 110133-07-8; $(CO)_4Cr(CHOH)_2$, 112069-49-5; $(CO)_4Mo(C(NH_2)_2)_2$, 112137-50-5; $H_2Pt(CH_2)_2^{2-}$, 112069-50-8.

Molecular Orbital and Spectroscopic Studies of Triple Bonds between Transition-Metal Atoms. 3.[1] The d^5–d^5 Organometallic Dimer $Re_2(C_3H_5)_4$

F. Albert Cotton* and George G. Stanley[2a]

Department of Chemistry, Texas A&M University, College Station, Texas 77843

Alan H. Cowley and Michael Lattman[2b]

Department of Chemistry, University of Texas, Austin, Texas 78712

Received May 19, 1987

The valence electronic structure of the organometallic dimer $Re_2(\eta^3\text{-}C_3H_5)_4$ which formally has a Re–Re bond order of 3 has been investigated by using molecular orbital theory and photoelectron spectroscopy. Relativistic SCF–Xα–SW calculations have been performed on $Re_2(\eta^3\text{-}C_3H_5)_4$ and a Re–Re triply bonding electronic configuration of $\sigma^2\pi^4\delta^2\delta^{*2}$ was found in agreement with previous Xα calculations on the d^5–d^5 Re(II) dimer $Re_2Cl_4(PH_3)_4$ and Fenske–Hall calculations on the model system $Tc_2(allyl)_4$. The calculation clearly indicates that a substantial amount of metal to ligand π back-bonding is occurring, primarily via interaction of the filled Re δ and δ^* orbitals with the energetically accessible allyl π^* levels. The significant differences between the molecular structures observed for $M_2(allyl)_4$ (M = Cr, Mo) and $Re_2(allyl)_4$ most likely result from the electronic factors favoring increased π back-donation in the Re system. The He I photoelectron spectrum for $Re_2(\eta^3\text{-}C_3H_5)_4$ is presented, and assignments from the Xα–SW calculation are proposed. Comparisons with the photoelectron spectra for the isoelectronic Re(II) dimer $Re_2Cl_4(PMe_3)_4$ and the quadruply bonded molybdenum dimer $Mo_2(allyl)_4$ confirm the predicted Re–allyl π back-donation.

There has been a great deal of research directed toward understanding the synthetic chemistry, structure (molecular and electronic), and reactivities of transition-metal multiple bonds.[3] Although there is a very large number of dimers with metal–metal triple and quadruple bonds, the list of organometallic binuclear systems with multiple bonds is much smaller. The quadruply bonded octamethyldimetalate species, $M_2(CH_3)_8{}^{x-}$, have been characterized for chromium,[4] molybdenum,[5] tungsten,[6] and rhenium.[7] Another homoleptic series of organometallic compounds with quadruple M–M bonds are the $M_2(\mu_2,\eta^8\text{-}C_8H_8)(\eta^4\text{-}C_8H_8)_2$ cyclooctatetraene-based dimers which are known for M = Cr, Mo, and W.[8–10] All three molecules are essentially isostructural, with the Mo and W compounds being crystallographically isomorphous.

The first "all organometallic" dimer crystallographically characterized was dichromium tetraallyl, $Cr_2(C_3H_5)_4$, which was found to have two terminal and two bridging allyl ligands, and, although it was not recognized at the time, a M–M quadruple bond with a Cr–Cr separation of 1.98 (6) Å.[11] As with the other systems discussed above, the isostructural molybdenum system has also been prepared, while the tungsten analogue is, as yet, unknown.[12] Interestingly, there is a related Re(II) complex, $Re_2(\eta^3\text{-}C_3H_5)_4$, which has a $\sigma^2\pi^4\delta^2\delta^{*2}$ electronic configuration corresponding to a Re–Re triple bond. The rhenium complex, however, has a rather different molecular structure from that observed for the related Cr and Mo systems.[13] The structure of the Cr/Mo complex is shown schematically in I, while ORTEP plots of the $Re_2(\eta^3\text{-allyl})_4$ complex are given in Figure 1. The Cr/Mo dimers have two bridging

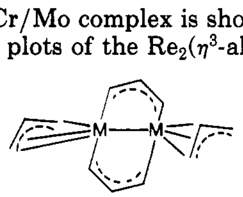

I

---

[1] Previous paper in series: Bursten, B. E.; Cotton, F. A.; Fanwick, P. E.; Stanley, G. G.; Walton, R. A. *J. Am. Chem. Soc.* **1983**, *105*, 2606.

[2] Current addresses: (a) Louisiana State University, Baton Rouge, LA 70803. (b) Southern Methodist University, Dallas, TX 75275

[3] Cf.: Cotton, F. A.; Walton, R. A. *Multiple Bonds Between Metal Atoms*; Wiley: New York, 1982.

[4] Krausse, J.; Marx, G.; Schödl, G. *J. Organomet. Chem.* **1970**, *21*, 159.

[5] Cotton, F. A.; Troup, J. M.; Webb, T. R.; Williamson, D. H.; Wilkinson, G. *J. Am. Chem. Soc.* **1974**, *96*, 3824.

[6] (a) Collins, D. M.; Cotton, F. A.; Koch, S.; Millar, M.; Murillo, C. A. *J. Am. Chem. Soc.* **1977**, *99*, 1259. (b) Cotton, F. A.; Koch, S.; Mertis, K.; Millar, M.; Wilkinson, G. *J. Am. Chem. Soc.* **1977**, *99*, 4989. (c) Collins, D. M.; Cotton, F. A.; Koch, S.; Millar, M.; Murillo, C. A. *Inorg. Chem.* **1978**, *17*, 2017.

[7] Cotton, F. A.; Gage, L. D.; Mertis, K.; Shive, L. W.; Wilkinson, G. *J. Am. Chem. Soc.* **1976**, *98*, 6922.

[8] Brauer, D. J.; Druger, C. *Inorg. Chem.* **1976**, *15*, 2511.

[9] Cotton, F. A.; Koch, S. A.; Schultz, A. J.; Williams, J. M. *Inorg. Chem.* **1978**, *17*, 2093.

[10] Cotton, F. A.; Koch, S. A. *J. Am. Chem. Soc.* **1977**, *99*, 7371.

[11] Aoki, T.; Furusaki, A.; Tomiee, Y.; Ono, K.; Tanaka, K. *Bull. Chem. Soc. Jpn.* **1969**, *42*, 545.

[12] Cotton, F. A.; Pipal, J. R. *J. Am. Chem. Soc.* **1971**, *93*, 5441.

[13] Cotton, F. A.; Extine, M. W. *J. Am. Chem. Soc.* **1978**, *100*, 3788.

0276-7333/88/2307-0835$01.50/0

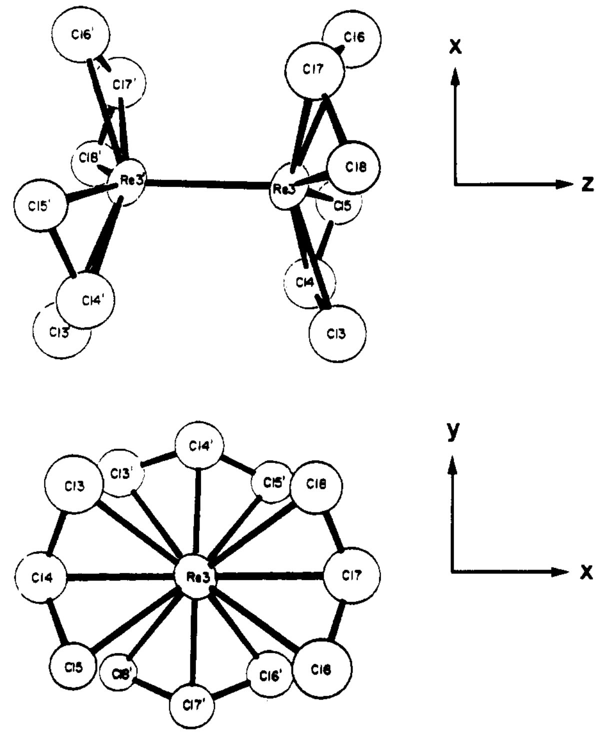

Figure 1. ORTEP plots of $Re_2(\eta^3\text{-}C_3H_5)_4$ showing view parallel and perpendicular to the Re–Re bond axis. Coordinate system for the Xα–SW calculation is also shown. Plots are from ref 13.

allyl groups and two terminally bound η^3-allyl moieties, while $Re_2(C_3H_5)_4$ possesses a more symmetrical D_{2d} structure with two η^3-allyl ligands bound to each metal center in a traditional fashion. The two types of Re–C distances are approximately the same with $Re\text{–}C_{out}$ = 2.22 (3) Å and $Re\text{–}C_{in}$ = 2.19 (2) Å; both are quite short compared to the $Mo_2(C_3H_5)_4$ structure where the Mo–C bond distances range from 2.24 (3) to 2.53 (2) Å, despite the presence of a smaller Mo atom.[12]

This startling difference in ligand coordination between two similar types of compounds most probably has an electronic rather than steric basis, since the difference in the Re–Re and Mo–Mo bond distances (0.042 Å longer for Re) is not expected to be large enough to make the bridging allyl mode of bonding unfavorable. Furthermore, the ^1H NMR spectrum of $Re_2(C_3H_5)_4$ in solution is consistent with the structure observed in the solid state, ruling out crystal packing forces as a cause for the differences in ligand geometries. While probing the electronic structure in the low-symmetry Cr or Mo allyl complexes by MO calculations would be a fairly difficult task, the higher symmetry of the rhenium system makes it a tractable complex in which to examine electronic effects, not only for the M–L bonding but also as a representative case for M–M bonding in an organometallic system. In this paper we report the results of relativistic SCF–Xα–SW molecular orbital calculations and He I photoelectron spectrum (PES) on $Re_2(\eta^3\text{-}C_3H_5)_4$. Although the electronic structure of this system has been probed previously by using the Fenske–Hall MO technique on a model technitium system,[13] we feel that the present SCF–Xα–SW calculation which includes relativistic effects, coupled with the experimental PES, will present a more accurate picture of the electronic structure of $Re_2(\eta^3\text{-}C_3H_5)_4$.

Computational and Experimental Section

SCF–Xα–SW Calculation on $Re_2(C_3H_5)_4$. A SCF–Xα–SW program package which included relativistic mass-velocity and Darwin corrections developed by Wood and Boring[14] was used on an Amdahl 470 V/6 computing system to calculate the ground-state electronic structures. Schwartz's α_{HF} atomic exchange parameters were used with the rhenium α value extrapolated as 0.693 16.[1,15] A valence electron weighted average of the atomic α values was used for the inter- and outer-sphere regions. Overlapping atomic sphere radii were taken as 89% of the atomic number radii calculated by the molecular superposition program.[16] All radii so used were found to be satisfactory and were not further optimized. The outer-sphere radius was made tangential to the outermost atomic sphere. Ionization potentials were calculated by using Slater's transition-state formalism that takes into account second-order relaxation effects.[17]

Bond distances and angles were taken from the crystal structure of $Re_2(\eta^3\text{-}C_3H_5)_4$ and averaged to conform to D_{2d} idealized symmetry.[13] The positions of the hydrogen atoms were estimated with the hydrogen atom on the central carbon atom, C1, in the plane of the allyl and on the bisector of the C2–C1–C2 angle (i.e., a sp^2-hybridized carbon). The outer C2 atoms were also taken as being essentially sp^2 hydridized, but with the carbon p orbital directed at the Re atom and not lined up for the traditional π bonding with the central C1 atom. This was based on the stereochemical requirements of Re–C2 bonding and hydrogen placement and agrees with the observed hydrogen atom positions in $Mo_2(C_3H_5)_4$.[12] The bond distances and angles used are Re–Re = 2.220 Å, Re–C1 = 2.162 Å, Re–C2 = 2.196 Å, C1–C2 = 1.41 Å, C–H = 1.00 Å, Re–Re–C1 = 98.2°, Re–Re–C2 = 110.2°, C2–C1–C2 = 123.4°, H–C2–H = 120°, and C2–C1–H = 118°. The initial molecular potential was constructed from Re (+2.0) and C (−0.333) atomic potentials along with the H 1s radial function. Sphere radii used are as follows: Re, 2.5587 au; C1, 1.6623 au; C2, 1.6968 au; H1, 1.1992 au; H2, 1.2028 au; H3, 1.2002 au; the outer sphere, 7.9128 au. A Watson sphere with a charge of +1.0 was used, and it was made 1 au larger than the outer-sphere radius. The Watson sphere was needed to artificially stabilize the energy levels and keep the calculation from oscillating. We believe that the electron-rich nature of the Re centers coupled with the considerable amount of inter-sphere charge density tends to produce instabilities in the Xα–SW calculational procedure. Since the energies from the Xα–SW technique are not absolute, the use of a Watson sphere serves mainly to apply a stabilizing electrostatic field to the overall molecular potential.

In spite of the use of the Watson sphere, the SCF calculation was very sensitive to the amount of new/old potential mixing and values no larger than 5% were used. Even so, 95 iterations were required to reach convergence, defined as <0.0050 Ry shift in the difference between potentials. This corresponded to a shift of less than 0.0001 Ry in any of the energy levels. A typical relativistic iteration took 64 s of CPU time.

Photoelectron Spectra of $Re_2(C_3H_5)_4$. The He I photoelectron spectra was run on a Perkin-Elmer PS-18 instrument and calibrated with xenon and argon reference ionizations. The approximate upper instrumental resolution was 40 meV. A typical temperature range used was 180–200 °C.

Results and Discussion

The results of the Xα–SW calculation on $Re_2(\eta^3\text{-allyl})_4$ are presented in Figure 2 and Table I for the upper valence molecular orbitals. Figure 1 shows ORTEP plots parallel and perpendicular to the Re–Re axis with the coordinate system used for the calculation. The percent contributions shown in Figure 2 and discussed in the text are *not* the usual atomic sphere charge contributions listed in Table I but rather, because of the fairly large intersphere charges,

---

(14) Wood, J. H.; Boring, M. A. *Phys. Rev. B: Condens. Matter* **1978**, *18*, 2701.

(15) (a) Schwarz, K. *Phys. Rev. B: Solid State* **1972**, *5*, 2466 (b) Schwarz, K. *Theor. Chim. Acta* **1974**, *34*, 225.

(16) Norman, J. G. *Mol. Phys.* **1976**, *31*, 1191.

(17) (a) Slater, J. C. *Quantum Theory of Molecules and Solids. The Self-Consistent Field for Large Molecules and Solids*; McGraw-Hill, New York, 1974; Vol. 4, (b) Johnson, K. H. *Annu. Rev. Phys. Chem.* **1975**, *26*, 39.

Table I. Upper Valence Orbitals for $Re_2(\eta^3\text{-}C_3H_5)_4$ from the SCF–Xα–SW Technique

		% contribution[c]							% Re angular contribution[d]			
MO[a,b]	E, eV	Re	C1	C2	H1	H2,3	INT	OUT	s	p	d	f
$5b_1$	−3.297	15	1	8	0	1	34	41			95	5
$8b_2$	−3.608	4	2	3	0	0	47	44				
$9a_1$	−3.723	24	5	17	1	5	40	9	27	48	24	1
12e	−3.808	3	3	7	0	1	45	41				
11e	−4.007	34	15	14	0	2	24	10		3	90	7
$8a_1$	−4.073	2	3	4	0	0	47	44				
$7b_2$	−4.770	56	2	4	0	3	30	4		12	86	2
10e	−6.972	28	5	30	0	2	31	3		24	74	3
$7a_1$	−7.173	63	11	5	0	1	19	1	5		95	
$6b_2$	−7.963	54	2	15	1	1	26	1	13	2	84	
9e	−8.052	11	24	29	3	3	27	2		33	67	
$4a_2$	−8.422	45	1	32	0	1	19	1			99	1
$4b_1$	−8.886	48	1	28	0	1	20	1			100	
$5b_2$	−9.258	16	27	21	3	4	26	2	27	3	69	1
$6a_1$	−9.286	19	19	26	4	7	24	2	27	3	68	2
8e	−9.823	77	2	7	1	1	12	0		1	97	2
$5a_1$	−12.171	97	0	2	0	0	0	0	23	8	67	3
$3b_1$	−13.626	0	31	50	0	19	0	0				
$3a_2$	−13.652	0	28	50	0	22	0	0				
7e	−13.854	0	31	48	1	17	3	0				
6e	−14.229	4	24	34	12	23	0	2				
$2a_2$	−14.844	2	6	48	0	42	0	2				
$4b_2$	−14.911	10	24	29	13	20	2	2	36		62	2
5e	−14.947	1	5	48	0	44	0	2				
$4a_1$	−14.956	11	26	27	15	17	3	2	35	1	64	1
$2b_1$	−15.098	2	4	48	0	44	0	2				
$3b_2$	−15.974	2	17	40	7	32	1	1				
4e	−16.101	2	15	42	4	33	3	0				
$3a_1$	−16.499	3	15	39	5	31	7	1				

[a] Levels above −3.0 eV are diffuse orbitals with the majority of their charges located in the inter- and outer-sphere regions and are not listed here. [b] The HOMO is the 10e level. [c] INT = inter-sphere and OUT = outer-sphere charge contributions to the MO. C1 is the center carbon atom of the allyl ligand; C2 represents the *two* equivalent terminal allyl carbon centers; H1 is bound to C1, and H2,3 are the hydrogen atoms bound to C2. [d] Listed only for Re contributions greater than 10%.

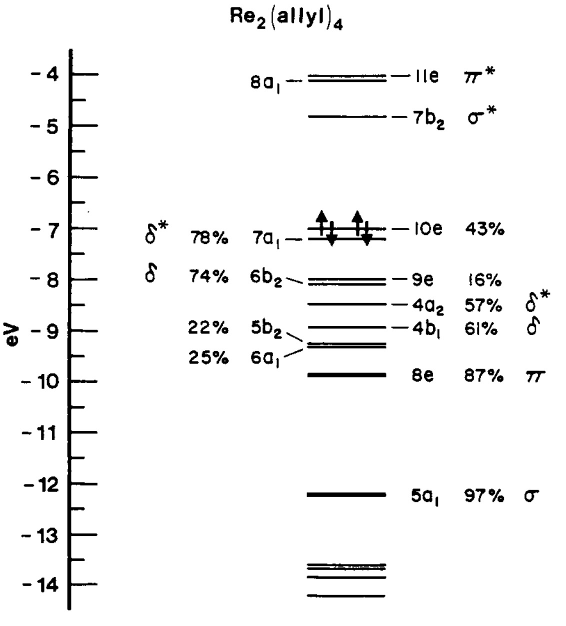

Figure 2. Molecular orbital diagram showing the upper valence orbitals from the SCF–Xα–SW calculation on $Re_2(\eta^3\text{-}C_3H_5)_4$. Highest occupied MO is indicated by arrows. Percent contributions are normalized Re atomic sphere contributions to the MO and are given only for occupied levels with 10% or greater Re character. Levels below the $5a_1$ are the allyl C–C and C–H bonding MO's.

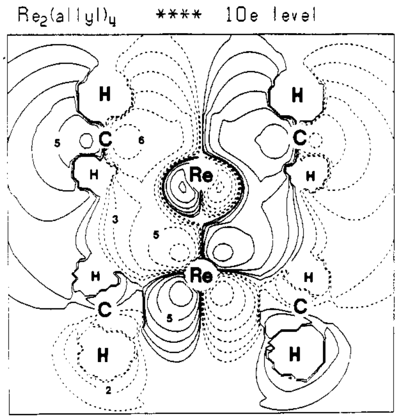

Figure 3. Contour plot of the 10e molecular orbital showing the dihedral plane. Dashed lines indicate negative contour values. Contour values used in all the plots are as follows: ±1, 0.0025; ±2, 0.005; ±3, 0.010; ±4, 0.020; ±5, 0.040; ±6, 0.080; and ±7 = 0.160 e/Å^3. Discontinuities in the plots are due to improper matching conditions at the atomic and outer-sphere boundries. They have no physical significance or effect on the calculations except to make sections of the contour plot look jagged.

normalized atomic charges which approximately take into account the inter- and outer-sphere charge densities by reproportioning them back onto the appropriate atomic spheres. this provides a crude alternative to what would, because of the relatively low D_{2d} symmetry and number of atoms, be a time consuming LCAO projection.[18] In referring to the carbon atoms, C1 will represent the middle carbon atom of the allyl ligand and C2 will be used for the two equivalent terminal carbon atoms. The contour diagrams shown are plots either in the *xz* plane, which contains the two rhenium atoms and two of the C1 allyl atoms, or in the plane lying 45° between the *xz* and *yz* planes which approximately cuts through the terminal C2 atoms.

---

[18] Bursten, B. E.; Jenson, J. R.; Fenske, R. F. *J. Chem. Phys.* **1978**, *68*, 3320.

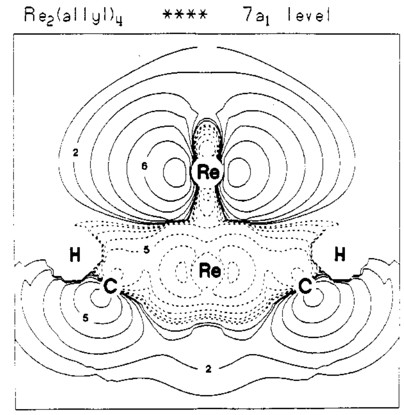

Figure 4. Contour plot of the $7a_1$ molecular orbital showing the xz plane.

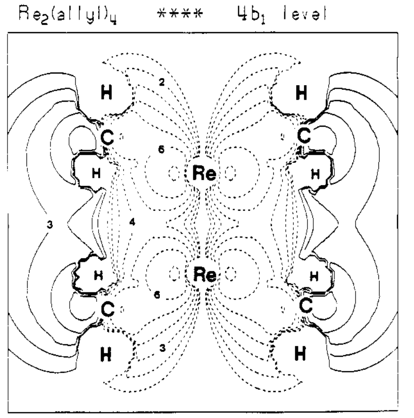

Figure 5. Contour plot of the $4b_1$ molecular orbital showing the dihedral plane.

The HOMO is the 10e level (Figure 3) which has a 43% Re contribution and is Re–C2 bonding, but Re–Re π^* antibonding. This, and the 9e orbital, are Re–C bonding levels. Because of the relatively high energy of the upper allyl π bonding (9e) and nonbonding (10e) levels, both MO's interact with the Re–Re π^* system giving rise to a type of ligand to metal back-bonding. The Re–Re π^* antibonding interaction is reduced somewhat by the presence of Re 6p character which hybidizes with the d_{xz} and d_{yz} orbitals, increasing the M–L bonding and reducing the amount of M–M antibonding π^* character.

The $7a_1$ (Figure 4) and $6b_2$ orbitals represent the Re–Re δ^* and δ interactions, respectively. In our previous calculations on $Re_2Cl_4(PR_3)_4$ the δ and δ^* orbitals were composed of Re d_{xy} AO combinations and the M–L bonding was via the Re $d_{x^2-y^2}$ AO's. The situation for $Re_2(\eta^3\text{-allyl})_4$, however, is reversed with the Re–Re δ and δ^* interactions now based on the $d_{x^2-y^2}$ AO combinations. As seen in Figure 1, the x and y axes used in the calculation pass through the middle carbon atoms (C1) of the allyl ligands so each Re $d_{x^2-y^2}$ orbital experiences M–L interactions only with the two C1 atoms while the d_{xy} orbital is directed at the four terminal C2 atoms. The stronger M–L interaction with the d_{xy} orbitals exchanges the respective functions of the d_{xy} and $d_{x^2-y^2}$ AO's, with the $d_{x^2-y^2}$ orbitals forming the δ and δ^* MO components. In marked contrast to "normal" δ and δ^* orbitals, they have substantial net bonding interactions with the C1 atoms of the allyl ligands which results in a donation of rhenium charge density into the allyl π^* antibonding orbitals. This allows the Re atoms to transfer electron density to the allyl π^* system, thus increasing the Re–C bonding while weakening the allyl C–C bonds. The $7a_1$ orbital, as shown schematically in II, has the ligand C1 and C2 percent contributions reversed from that seen for the $6b_2$ orbital. The $d_{z^2}/d_{x^2-y^2}$ hybridization on the Re atoms favors the Re–C2 interactions in both the $6b_2$ and $7a_1$ orbitals.

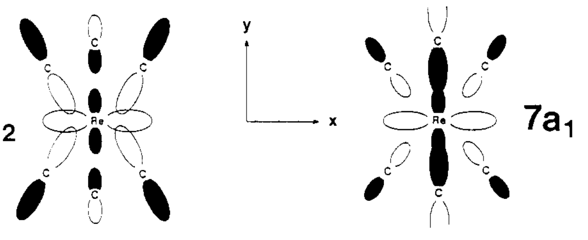

II

The $4a_2$ and $4b_1$ (Figure 5) MO's are strongly M–L bonding between the Re $d_{x^2-y^2}$ AO and the C2 allyl atoms. The large Re contribution (58%) indicates that a considerable amount of charge is being transferred from the allyl ligands to the metal atoms, similar to that seen in the Xα calculations for the $\sigma^2\pi^4$ M–M triply bonded complex, $Mo_2(CH_3)_6$[19] and implying a relatively strong covalent bonding situation. The $5b_2$ and $6a_1$ orbitals are also Re–C bonding, but not to the extent seen for the $4a_2$ and $4b_1$ MO's. Both the $5b_2$ and $6a_1$ orbitals have Re $6s/5d_{z^2}$ mixing which works to improve the M–L bonding and reduce the Re–Re σ and σ^* interactions also present in these orbitals. This hybridization is very similar to that seen in the $Re_2Cl_4(PH_3)_4$ and Mo_2L_6 calculations.[1,19]

The Re–Re bonding is concentrated in the 8e (π) and $5a_1$ (σ) orbitals which both have large Re contributions (8e, 87% Re; $5a_1$, 97% Re), indicating relatively pure M–M bonding MO's. The 8e level is essentially pure 5d in character, while the $5a_1$ is a $6s/5d_{z^2}$ combination with the σ mixing favoring the Re–Re σ bonding. The orbitals below the $5a_1$ level are the C–C and C–H bonding levels which will not be discussed further.

The Xα–SW technique does not give direct information about bond strengths or bond distance/angle optimizations because total energies are not reliably calculated. Qualitatively, however, the Re–C interaction appears to be quite strong since there are large metal contributions to several of the M–L bonding orbitals, particularly the $4a_2$ and $4b_1$ levels, and no M–L antibonding interactions of any significance in the occupied MO's. The allyl character in the M–L bonding orbitals comes from a combination of π and π-nonbonding based orbitals, with the π-bonding character mixing into the lower Re–C bonding MO's such as the $5b_2$, $6a_1$, and 9e levels. The higher energy allyl π-nonbonding MO's mix strongly into the $4a_2$ and $4b_1$ orbitals, as well as the 10e level. Furthermore, the availability of energetically accessible empty π^* levels on the allyl ligands provides a π-back-bonding mechanism for the Re atoms to transfer some of their excess electron density back onto the ligands. The donation of electron density from the allyl ligands into the Re–Re π^* MO is unusual in the sense that it occurs to such a large extent in the 10e orbital. The relatively short Re–Re triple bond distance of 2.225 (7) Å implies that either the calculation is overestimating the ligand to metal donation into the Re–Re π^* orbital or the strong Re–Re σ bonding and substantial involvement of Re 6p orbitals is compensating very effectively for the weakening of the Re–Re d orbital based π bonding.

Some evidence for the predicted strong Re–C bonding comes from the fairly short Re–C bond lengths of 2.22 (3)

---

[19] Bursten, B. E.; Cotton, F. A.; Green, J. C.; Seddon, E. A.; Stanley, G. G. *J. Am. Chem. Soc.* **1980**, *102*, 4579.

Table II. Calculated Ionization Potentials for $Re_2(\eta^3\text{-}C_3H_5)_4$

level	type[a]	IP[b] (eV)	level	type[a]	IP[b] (eV)
10e	Re–C	8.88	$3a_2$	C–C	(15.8)
$7a_1$	δ*	9.07	7e	C–C	(16.0)
$6b_2$	δ	9.85	6e	C–C	(16.3)
9e	Re–C	10.05	$2a_2$	C–H	(16.9)
$4a_2$	Re–C	10.55	$4b_2$	C–C	(17.0)
$4b_1$	Re–C	(11.0)	5e	C–H	(17.0)
$5b_2$	Re–C	11.28	$4a_1$	C–C	(17.1)
$6a_1$	Re–C	(11.3)	$2b_1$	C–H	(17.2)
8e	π	12.14	$3b_2$	C–H	(18.1)
$5a_1$	σ	14.67	4e	C–H	(18.2)
$3b_1$	C–C	(15.7)	$3a_1$	C–H	(18.6)

[a] Principal function of the orbital. [b] Values in parentheses are estimates from the calculated ionizations and should be accurate to approximately 0.1 eV for the higher energy values and 0.3 eV for the lower energy orbitals.

(Re–C2) and 2.19 (2) Å (Re–C1).[13] These can be compared to the longer Mo–C bond distances at 2.24 (2)–2.53 (3) Å in $Mo_2(allyl)_4$, despite the presence of a smaller molybdenum atom.[12] Not enough, however, is known about the thermodynamics or reactivities of these compounds to justify detailed comparisons. Similarly, the average C–C bond lengths, 1.44 (5) Å, of the allyl groups in $Re_2(allyl)_4$ appear to be longer than those seen in $Mo_2(allyl)_4$, 1.37 (2) Å, and a number of other transition-metal allyl compounds,[12] suggesting that the donation of considerable amounts of metal electron density into the allyl π* orbitals predicted by the Xα calculation could be real. Unfortunately, the large estimated standard deviations on the C–C bond distances in $Re_2(allyl)_4$, coupled with the variable effect of refinement of those distances with and without hydrogen atoms,[13] combine to invalidate detailed comparisons. The infrared spectrum of $Mo_2(allyl)_4$ has not been reported, but even if it had, the low symmetry of the molecule and resulting complexity of the IR spectrum would make comparisons of C–C stretching frequencies between the Mo and Re allyls a difficult affair.

One important piece of experimental data that we do have is the He I photoelectron spectrum (PES) of $Re_2(allyl)_4$, shown in Figure 6. The calculated ionization potentials IP's) are listed in Table II and in Figure 6 where they have been uniformly shifted to match up the first experimental and calculated peak values. It is clear from Figure 6 that the calculated IP's do *not* agree very well with the PES band structure, particularly if one considers the experimental intensity ratio of peaks A:B:C as 1:3.0:7.1, strongly suggesting that the assignment of both 10e and $7a_1$ levels to peak A is quite wrong. The poor agreement is due to the large inter-sphere charge contributions (see Table I) in the uppermost, mainly ligand π-based valence levels which artificially raises the energy of these MO's relative to the more localized metal-based levels. We have observed this same effet in Xα–SW calculations on $Cr_2(hydroxypyridine)_4$ and $Mo_2(CH_2PH_2CH_2)_4$ where large inter-sphere contributions, which originate from the ligand p and π orbitals, cause the upper ligand levels to shift approximately 2 eV above that of the M–M δ-bonding MO, even though in both cases the PES clearly shows that the HOMO must be the δ-bonding MO.[20,21]

When this information is combined with the peak intensity data, some reasonable assignments can be suggested. Peak A, therefore, is believed to arise from the ionization of the $7a_1$ Re–Re δ* orbital, while peak B results from the 10e allyl-based orbital and the $6b_2$ Re–Re δ-bonding level. Region C, which shows a good deal of substructure, arises from the $4a_2$, 9e, $4b_1$, $5b_2$, $6a_1$, and 8e MO's. The calculation intensity ratio, assuming these orbital assignments and simple intensity values of one and two for singly and doubly degenerate orbitals, is 1:3:8 for A:B:C, which compares well to the experimental ratio of 1:3.0:7.1. The lower IP's are calculated too low in energy, and we would assign the $5a_1$ Re–Re σ-bonding level in the −11.0 to −11.5 eV region with the C–C and C–H bonding levels making up regions D and E, respectively. The tendency for the Xα–SW technique to calculate the principal M–M σ bonding level too low was also seen for the $Re_2Cl_4(PH_3)_4$ system, although it does not seem to be quite as overestimated in this calculation.[1]

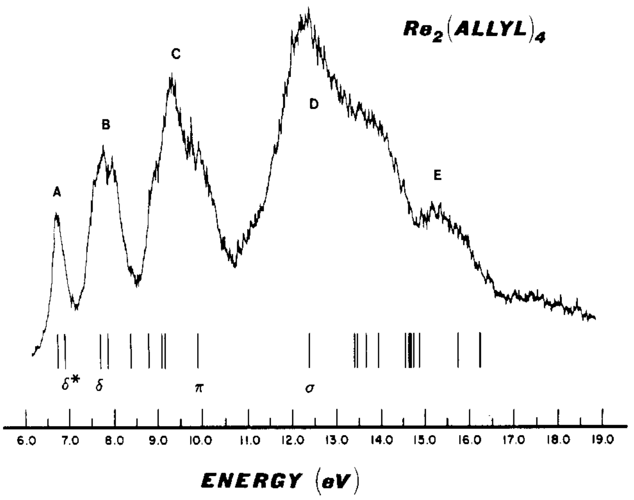

Figure 6. He I photoelectron spectrum for $Re_2(\eta^3\text{-}C_3H_5)_4$. Calculated ionization potentials from the Xα–SW calculation are shown shifted in energy to match the first level with the first experimental peak. Correct assignments are discussed in the text.

The previously reported Fenske–Hall molecular orbital calculation on the $Tc_2(allyl)_4$ model system agrees with the assignments presented above.[13] In fact, the results from the Fenske–Hall calculation are qualitatively better as far as the level ordering is concerned than those from the Xα–SW method (which suffers to a certain extent from the inter-sphere charge problem) with the Re–Re δ* orbital being the HOMO followed by the allyl π-nonbonding (10e) and Re–Re δ MO's. A group of ligand-based MO's mixed in with the Re–Re π- and σ-bonding levels form the next contingent of orbitals, followed by the allylic C–C and C–H σ orbitals. One difference between the calculations is in the amount of π-back-donation occurring from the metal atoms to the allyl ligands—the Xα–SW calculation indicates that quite a bit more back-bonding is occurring. As we will see, this will prove to be an important difference between the two calculations.

We can also compare these results with the PES data on the dichromium and dimolybdenum tetraallyl dimers that have been reported by Green and Seddon.[22] The PES of $Re_2(allyl)_4$ resembles that of $Mo_2(allyl)_4$, except, of course, with an additional peak at lower energies that corresponds to the δ* orbital that is unoccupied in the quadruply bonded chromium/molybdenum species. The M–M δ MO is located at 6.72 eV in $Mo_2(allyl)_4$ while the δ* orbital is located at 6.70 eV in $Re_2(allyl)_4$. While we do not have the He II PES to assist in picking out the ionizations with considerable rhenium character, the assignment of the allyl 10e level to larger peak B component at

---

(20) Bursten, B. E.; Cotton, F. A.; Cowley, A. H.; Hanson, B. E.; Lattman, M.; Stanley, G. G. *J. Am. Chem. Soc.* **1979**, *101*, 6244.

(21) Bursten, B. E.; Cotton, F. A.; Cowley, A. H.; Lattman, M.; Stanley, G. G., unpublished SCF-Xα-SW and PES results.

(22) Green, J. C.; Seddon, E. A. *J. Organomet. Chem.* **1980**, *198*, C61.

7.7 eV and the Re–Re δ-bonding MO to the feature at 7.9 eV would seem most reasonable from an intensity viewpoint.

The δ–δ^* separation based on this assignment is 1.2 eV, which fits well with the δ–δ^* separation of 0.85 eV seen in the PES of $Re_2Cl_4(PMe_3)_4$ by Lichtenberger and coworkers.[23] The somewhat larger δ–δ^* separation seen in $Re_2(allyl)_4$ may be related to the considerable mixing of allylic character into the δ orbitals. This type of ligand mixing into the M–M δ and δ^* levels is not seen in "traditional" dimers such as $Re_2Cl_4(PMe_3)_4$ and is one of the unique aspects of this system. The relatively narrow shape of peak A also supports the formulation of this ionization as the Re–Re δ^* orbital, analogous to that observed in the $Re_2Cl_4(PMe_3)_4$ system.[23] The shifting of the Re-based ionizations to higher ionization potentials is fully consistent with the higher electronegativity and increased effective nuclear charge of Re relative to Mo and has been previously observed in the comparison of the PES spectra of $Re_2Cl_4(PMe_3)_4$ and $W_2Cl_4(PMe_3)_4$.[23] This shifting of the Re ionizations to higher IP's also accounts for the merging of the Re δ and allyl ionizations in band B, while in $Mo_2(allyl)_4$ the Mo–Mo δ band is separated from the allyl levels by 0.9 eV. The assignments of the Re–Re π level to band C and the Re–Re σ-bonding level to the leading edge of peak D is also consistent with the assignments proposed for $Mo_2(allyl)_4$ and $Re_2Cl_4(PMe_3)_4$. The separations between the $\delta/\pi/\sigma$ ionizations are as follows: $Re_2Cl_4(PMe_3)_4$ (δ–π = 1.4 eV, π–σ = 0.9 eV) and approximate values for $Re_2(allyl)_4$ (δ–π = 1.0–1.9 eV, π–σ = 1.4–2.4 eV).

The photoelectron spectra may also be giving us important data concerning the presence of considerale Re–allyl π back-bonding predicted by the Xα–SW calculation. The position of the δ and δ^* ionizations in $Re_2Cl_4(PMe_3)_4$ are located at 5.66 and 6.51 eV, respectively,[23] while the δ–δ^* ionizations in $Re_2(allyl)_4$ are found at considerably higher IP's of 6.70 and 7.7–7.9 (7.9 based on our tentative assignment) eV. The shifting of these Re–based orbitals to higher IP's by approximately 1.1 eV clearly points to the fact that there is *less* electron density on the Re atoms in $Re_2(allyl)_4$ relative to $Re_2Cl_4(PMe_3)_4$. From a molecular orbital aspect the displacement of the δ and δ^* to higher IP's corresponds *exactly* to the stabilization of these orbitals by π^* back-bonding. It is important to remember that $Re_2(allyl)_4$ and $Re_2Cl_4(PMe_3)_4$ are isoelectronic neutral Re(II)–Re(II) dimers, so direct comparisons between them are most instructive. Although one might be willing to argue which ligand set constitutes a better donor set, Cl^-/PMe_3 or allyl$^-$, the primary electronic difference between these ligands is the known and well-established π^* back-bonding ability of the allylic (and other π systems) ligand. The shifting of the Re–Re δ and δ^* ionizations to higher IP's provides compelling experimental evidence supporting the Xα–SW calculational results which clearly show considerable back-donation of Re electron density to the allylic π^* orbitals.

Careful comparison of the PES of $Re_2(allyl)_4$ and $Mo_2(allyl)_4$ also offers subtle evidence for the presence of increased Re–allyl π^* back-bonding. If there is a significant amount of π back-donation to the allylic ligands reducing the electron density on the rhenium atoms but increasing the density on the carbon atoms, then one might expect to see shifting of the allylic ionizations in the PES spectrum toward *lower* ionization potentials. We do indeed see such a change with the deeper allyl C–C and C–H ionizations shifted to lower IP's by about 0.8 eV. The band shape of this region (peaks D and E in our PES), however, does not change appreciably, indicating that this effect is related to an overall increase in the electron density on the allylic ligands as opposed to some specific perturbation on the C–C and C–H σ framework. Peak C in our spectrum, which is composed of Re–C and Re–Re π-bonding levels, is also shifted to lower ionizations relative to the same peak in the PES of $Mo_2(allyl)_4$ (also labeled peak C) by ca. 0.8 eV.

Despite the lack of quantitative agreement, the Xα–SW results provide a valuable guide to the assignment of the PES that is consistent with the observed peak structure and relative intensities. The PES of $Re_2(allyl)_4$ and $Re_2Cl_4(PMe_3)_4$ would appear to confirm the presence of considerable amounts of Re–allyl π back-donation based on the shifting of the Re ionizations to higher IP's and the allyl levels to lower IP's. The calculation also offers insight into the details of the M–M and M–L bonding. While we cannot state with certainty the reason for the significant differences in structure between the Cr/Mo and Re allyl dimers, it would appear that the greater electron density on the Re(II) atoms and the presence of a filled Re–Re δ^* orbital combine with the π back-donation into the very accessible allyl π^* orbitals to make a major electronic difference in the rhenium complex. The orientation of the allyl ligands in the Re dimer allows a much better interaction with the formally localized and electron-rich Re–Re δ and δ^* orbitals to give the best π back-bonding to the allyl ligands.

Acknowledgment. We wish to thank the National Science Foundation for research support, Prof. Bruce E. Bursten (Ohio State University) for assistance with the Xα program set, and Prof. Dennis Lichtenberger (University of Arizona) for extremely helpful reviewer comments.

Registry No. I, 65836-68-2; Re, 7440-15-5.

---

[23] Root, D. R.; Blevins, C. H.; Lichtenberger, D. L.; Sattelberger, A. P.; Walton, R. A. *J. Am. Chem. Soc.* **1986**, *108*, 953.